Detection-Localization-Identification of Vibrations over Long Distance SSMF with coherent $\Delta\phi$-OTDR

Elie Awwad, *Member, IEEE,* Christian Dorize, Sterenn Guerrier and Jérémie Renaudier, *Member, IEEE*

(Extended ECOC'19 paper, Invited Paper)

***Abstract*—We propose a novel interrogation technique for Distributed Acoustic Sensing (DAS) and demonstrate the detection and recognition of multiple vibration events over 50km of SSMF. A differential-phase optical time-domain reflectometry ($\Delta\phi-$OTDR) approach is used. At the transmitter side, a continuous ultra-narrow-linewidth laser is modulated with polarization-multiplexed orthogonal binary sequences and at the receiver side, the back-scattered signal is captured through a polarization-diversity coherent mixer in a self-homodyne configuration. The detection of the full optical field vector and the use of an ultra-narrow-linewidth laser source enhance the sensitivity of the interrogating solution. A comparison of the experimental results to a simulation model is developed to better understand the noise limits. A low-complexity localization technique based on a multi-resolution approach is also presented. Major results include the identification of an engine noise, paving the way for numerous smart-city/industrial monitoring applications over deployed telecom fibres.**

***Index Terms*—Optical fibre sensors, optical fibre networks.**

I. Introduction

OPTICAL fibre sensing over deployed telecom infrastructure is emerging as a hot topic to enable enhanced monitoring capabilities for operators and smart-city applications such as road traffic surveillance [1], railway surveillance [2], earthquake detection [3]. The enabling technology is known as distributed acoustic sensing and is based on Rayleigh-OTDR (optical time domain reflectometry) with a coherent laser source. The fibre imperfections (scatterers) randomly distributed in the core induce a backscattering of $-70\mathrm{dB/m}$. When light is sent from a coherent laser source into a fibre, a coherent speckle pattern over the covered fibre distance is detected from the backscattered light [4]. When a vibration impacts the fibre, the induced intensity variations (amplitude-based DAS [5], [6]) or phase variations (differential-phase DAS [7]) are spotted to localize and identify the vibration source. These variations are caused by micro- or even nano-extensions/contractions of the fibre that move the scatterers which causes changes of the backscattered interference pattern. Phase-based schemes can offer an enhanced sensitivity as well as a linear response giving them an advantage over amplitude-based interrogation. By linearity, we refer to the relation between the applied strain and the induced phase change; however, we keep in mind the non-linearity that can arise from phase unwrapping operations [7].

E. Awwad was with Nokia Bell Labs France and is now with the Department of Communications and Electronics of TELECOM Paris, 16 place Marguerite Perey, 91120 Palaiseau, e-mail: elie.awwad@telecom-paris.fr

C. Dorize, S. Guerrier and J. Renaudier are with Nokia Bell Labs France, route de Villejust, 91620 Nozay.

Manuscript received Nov 15, 2019; revised XXX MM, YYYY.

In this work, we build upon phase-based coherent DAS technology [8] and enhance it by replacing single-pulse interrogation with continuous transmission of two probing sequences multiplexed over two orthogonal polarization states of the light signal injected in the sensed fibre. We also use at the receiver side a dual-polarization coherent mixer to detect the backscattered light that beats with a local oscillator in a self-homodyne configuration. In this approach, the detected signal does not directly reflect the fibre response which has to be extracted from it through a correlation process with the transmitted sequences as explained in [9]. The multiple-input multiple-output (MIMO) approach through polarization multiplexing at the transmitter and polarization-diversity detection at the receiver side offers robustness to polarization fading [10] and enables the supervision of the state of polarization in addition to the intensity and common phase.

The probing sequences consist of two mutually orthogonal Golay binary pairs mapped to binary- or quaternary-phase-shift-keying (BPSK/QPSK) symbols that jointly and continuously modulate two orthogonal polarization states of a narrow-linewidth laser source. A perfect estimation of the fibre response is obtained in the form of Jones matrices from which optical phase variations in time are derived per fibre segment. The method was experimentally validated with large bandwidth acoustic signals over a 100m long fibre equipped with fibre Bragg Gratings to enhance the backscattered intensity [11]. The present paper is an extended version of [12], it aims to extend the scope of the probing method to long distances over standard single mode fibres (SSMF). We assess the performance in terms of sensitivity and bandwidth through experiments and a developed simulation model. Through our experimental demonstrations, we potentially target distributed sensing over the widespread networks of deployed telecom fibres, and address the identification and localization of a variety of vibration events in smart city monitoring applications (transportation, industries, security...).

The paper is organized as follows. Section II details the probing method that enables perfect channel estimation and the associated processing at the receiver side consisting mainly of a correlation process and a low-complexity event identification and localization procedure. In section III, we describe a Rayleigh back-scattering model in static conditions used to determine the noise limits of the proposed interrogation scheme and to understand the reach limit over which vibrations can be captured in an SSMF. Section IV describes the experimental setup and finally section V details the experimental results highlighting the ability to detect and identify synthetic signals along a 51 km SSMF up to the fibre end.

II. Fibre response estimation & information extraction

A. Probing method

In baseband, the polarization-division-multiplexed (PDM) field vectors generated at the transmitter side at $F_s = 1/T_s$ are given by:

$$\mathbf{E_t}(n) = \begin{pmatrix} A_{tx}(n) \\ A_{ty}(n)) \end{pmatrix} \quad (1)$$

where $n = [1...N]$ is a time index, $A_{tx,ty}(n) \in \{-1; 1\}$ are binary phase shift keying symbols (BPSK) chosen from two mutually orthogonal Golay pairs as explained in [9] to guarantee a perfect channel estimation. We intentionally restricted the design of the probing sequences to binary symbols to avoid the use of complex modulation formats that are less tolerant to transmitter imperfections.

The Rayleigh back-scattered signal captured at the dual-polarization coherent receiver does not immediately provide the fibre response as in the single-pulse periodic interrogation. It rather consists of a superposition of all the back-scattered symbols. The channel response should be extracted through a correlation process between the two received symbol-vectors and the two emitted symbol-vectors. The specific orthogonality properties between the designed sequences guarantee the perfect channel estimation provided that a suitable sequence length is chosen. The length of the sequence depends on the mapping between the complementary Golay codes and the chosen modulation format [9]. In the case of BPSK-coded symbols, the probing code length $T_{code} = N_{code}/F_s$, where N_{code} is the number of symbols, should satisfy $T_{code} > 4T_{ir}$ to avoid the overlap of the channel response with the correlation noise [9]. $T_{ir} = 2L/c_f$ stands for the time spreading of the channel response for a fibre of length L, c_f being the velocity of light in the core of the fibre, N_{code} is typically a power of 2 and the generation process is detailed in [9].

After correlation with the transmitted sequences, we obtain $\mathbf{E_r} = \mathbf{H_{i,j}}\mathbf{E_t}$ where $\mathbf{E_r} = \{E_{rx}; E_{ry}\}$ stands for the optical field back-scattered from the i^{th} fibre segment at time index j. The 2×2 Jones matrix $\mathbf{H_{i,j}}$ is the dual-pass impulse response from the start of the fibre to the i^{th} fibre segment at time index j. $\mathbf{H_{i,j}}$ is estimated for each fibre segment index i whose length $S_r = c_f/(2F_s)$ is determined by the symbol rate F_s of the transmitted probing sequence. The probing codes are repeated with a period equal to the code duration T_{code}, leading to periodic estimations of $\mathbf{H_{i,j}}$. We define the mechanical bandwidth of the interrogator as $BW = 1/(2T_{code})$. Vibrations below BW-Hz can be perfectly detected.

B. Low-complexity information extraction method

$\mathbf{H_{i,j}}$ contains all the information on the transformation endured by the optical field from the interrogator up to a given location in the fibre and back to the interrogator. This information includes the change in the polarization state, the common phase term and energy of the optical field. All three metrics are susceptible to react to an applied strain on the fibre coming from a neighboring vibration source for instance. In this work, we will focus on the changes of the optical phase term known to change linearly with respect to the applied strain $\Delta\Phi = 4\pi n\xi/\lambda\Delta L$ where n is the refractive index of the fibre core, λ is the probing channel wavelength, $\xi = 0.78$ is the photo-elastic scaling factor for a longitudinal fibre strain and ΔL the longitudinal strain induced by the fibre [13].

The optical phase is estimated as $\Phi_{i,j} = 0.5\angle det(\mathbf{H_{i,j}})$ where $det()$ stands for the determinant operator. The differential phase in the spatial dimension is then computed to obtain its evolution of the optical phase in time for each spatial segment. The phase standard deviation (StDv) in time is used as a metric for monitoring the interrogated fibre. In static conditions, the phase variations will be dictated by the laser phase noise observed by the optical field both at the modulation step and at the coherent detection step, hence a high-coherence laser source is required to guarantee low phase noise. In presence of mechanical perturbations, these will be detected and localized from the magnitude and position of peaks emerging in the differential phase StDv along the sensed fibre.

Considering a 50-km long fibre that needs to be monitored with a gauge length of 1m or finer, this requires the constant monitoring of 50000 spatial segments at least: a considerable amount of data that becomes the main bottleneck for real-time monitoring applications. Hence, we proceed in a multi-resolution iterative approach [14] that consists in a coarse localization of mechanical events using a subset of high-reflecting fibre segments, followed by a low complexity localization refinement. Indeed, the intensity of the obtained interference pattern from the Rayleigh back-scattered signal when sending light from a high-coherence laser source, usually called 'speckle' pattern, has large dynamics [4]. The scattered fields from individual scattering points in a given fibre segment can add up destructively or constructively depending on their phase and amplitude relations.

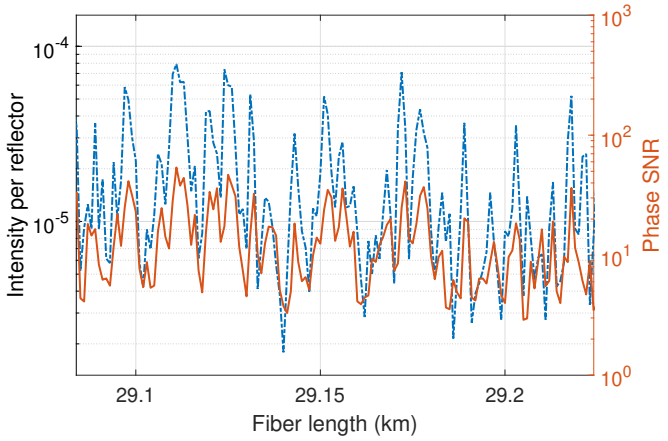

Fig. 1. Back-scattered Rayleigh intensity pattern & inverse standard deviation of phase per segment in static mode around 29.1km.

The procedure consists in a permanent monitoring of phases running continuously over a subset of fibre segments. This subset is defined based on the backscattered intensity levels measured in static mode as shown in Fig. 1. Normalized intensity levels measured at the native gauge length are shown over a fibre section at 29.1km from the interrogator. Super-

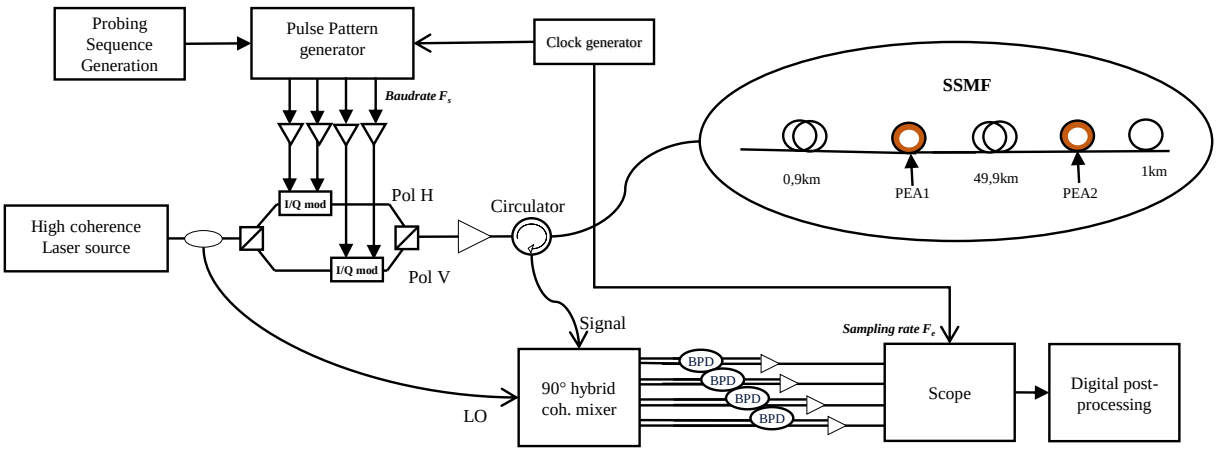

Fig. 2. Experimental Setup (PEA: Piezoelectric actuator, Pol: polarization, BPD : balanced photodetectors).

imposed on the intensity curve is the inverse of the standard deviation of the differential phases per fibre segment (dashed line) estimated over 1s with a 1ms-long probing code in static conditions. We can clearly see that the higher the scattered intensity, the lower the phase variations are (better signal-to-noise ratio). Based on this observation, we perform a selection of segments at a low spatial resolution $S_{coarse} = LS_r$ by keeping the highest-reflecting segment among L adjacent ones. The differential phases are extracted from this subset. If a single or multiple perturbations are detected through the appearance of peaks in the StDv of the differential phases, local analyses are triggered over the segment(s) preceding the perturbed one(s) at a higher resolution to accurately localize the event(s). The spatial resolution increase may be applied consistently until we end up localizing the event(s) with the native gauge length S_r. This procedure will be illustrated in section V.

III. Rayleigh backscattering model

In order to understand the sensitivity limits of the interrogator in static mode (no perturbations applied on the fibre, the only existing noise is generated by the interrogator itself), we developed a dual-polarization model of the Rayleigh back-scattering [15] including a spatial discretization of an SSMF fibre reflecting the segmentation induced by the interrogation at a given symbol rate. The fibre is described as an array of uniformly distributed scattering centers of random amplitudes (Normal distribution around the mean Rayleigh back-scattering coefficient). This yields a scalar response in amplitude and phase e_i for each fibre segment [16]. For the polarization evolution, we use a Jones formalism with a unitary matrix $\mathbf{U_{fwd,i}}$ randomly drawn to represent the polarization rotation in the forward propagation from the interrogator to segment i, a reflection matrix $\mathbf{M_i} = \begin{pmatrix} \sqrt{1-\alpha} & \sqrt{\alpha} \\ \sqrt{\alpha} & -\sqrt{1-\alpha} \end{pmatrix}$ with $\alpha = 0.05$ considering that 5% of the back-scattered intensity emerges into an orthogonal polarization state [17] , and a backward propagation matrix $\mathbf{U_{bwd,i}} = \mathbf{U_{fwd,i}^{\dagger}}$ since the optical fibre is reciprocal. Hence, we model $\mathbf{H_i}$ the round-trip channel up to the i^{th} segment as $\mathbf{H_i} = e_i \mathbf{U_{fwd,i}}^{\dagger} \mathbf{M_i} \mathbf{U_{fwd,i}}$. The full back-scattered field is then given by:

$$\mathbf{E_{out}} = \sum_i e_i \mathbf{U}_{forward,i}^{\dagger} \mathbf{M} \mathbf{U}_{forward,i} \mathbf{E}_{in} \qquad (2)$$

Apart from the fibre model, the emission and reception stages are also emulated. Laser phase noise was added at both stages at the modulation step and at the local oscillator. The phase noise is modeled as a Wiener process of variance $\sigma^2 = 2\pi\Delta\nu T_S$ where $\Delta\nu$ is the laser linewidth. Transmitter and receiver noises and losses are also taken into account with parameters extracted from the datasheet of the components used in the experimental setup. We typically modeled relative intensity noise of the laser, thermal noise at the driver and trans-impedance amplifiers, and shot noise at the photodiodes. We draw 50 random polarization states of a 50km-long fibre segmented with a resolution of 2m, study the noise impact on the estimated phases and compare the results to the experimental measurements which will be shown later in section V.

IV. Experimental setup

The setup is presented in Fig. 2. The probing signals are sent on two orthogonal polarizations through a dual-polarization 25GHz I/Q Mach-Zehnder modulator ($F_{symb} = 50$MBaud) to modulate the optical wavelength. The figure shows the general case of an I/Q modulation, however we restrict ourselves in this work to a BPSK modulation per polarization. The modulated signal is then amplified to an average power of 5dBm and sent through a circulator into the sensed fibre. The Rayleigh back-scattered signal goes through the circulator to a dual-polarization coherent mixer. The in-phase and quadrature information of the signal projection over two orthogonal polarization states are captured by 1.6GHz 3dB-bandwidth balanced photodiodes and amplified by trans-impedance amplifiers. The four captured signals are then sampled at $2F_s = 100$MSamples/s using a 12-bit resolution scope. Offline signal processing is carried over the acquired sequences, starting with power normalization, followed by a correlation with the transmitted sequences to periodically extract the fibre response given by a series of 2×2 Jones matrices separated with a gauge

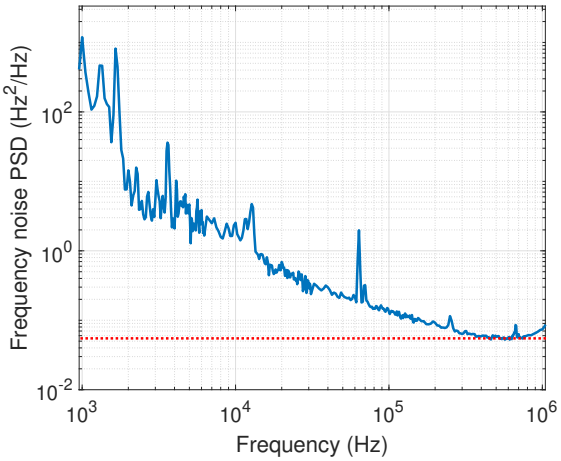

Fig. 3. Measured frequency noise spectrum of the laser source through a self-heterodyne linewidth measurement setup.

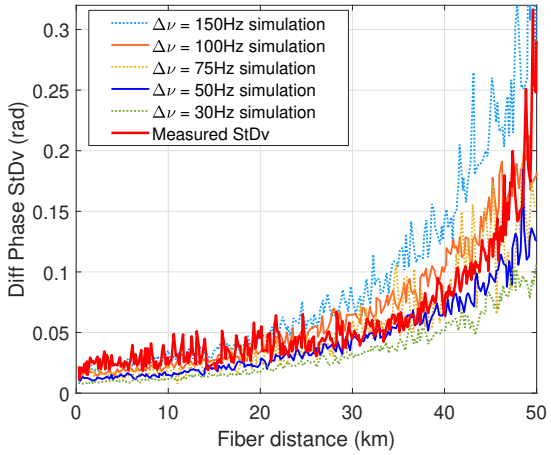

Fig. 4. Phase standard deviation as a function of distance in static mode (simulations for various laser linewidth values and the experimental result).

length $S_r = 2$m imposed by the symbol rate $F_s = 50$MBaud. A time synchronization is then applied to detect the periodic responses with a period of T_{code}. The differential phases are then extracted and monitored following the multi-resolution procedure presented in section II.

An overall 52km-long SSMF link is sensed. Two mechanical perturbations are applied, the first one at approximately 0.9km and the second at approximately 50km from the interrogator. We use cylindrical piezoelectric actuators (PEA) with an outer diameter of 5cm to apply strain on bare fibres. The first actuator (PEA1) has 55cm of fibre coiled around it while the second one (PEA2) has 133cm. These actuators are fed with electrical signals. The signal generated for the experiment presented in the next section is a combination of tones which emulates an engine noise, used to demonstrate localization of different events as well as identification from spectral analysis.

An OEwaves^{TM} ultra-low-linewidth laser emitting 10dBm at $\lambda = 1536.6$nm is used as a source at the transmitter and a local oscillator at the receiver, with a given Lorentzian linewidth inferior to 1Hz in a 10μs window according to its specifications sheet. We characterized the frequency noise spectrum of the laser through a self-heterodyne linewidth measurement with a 100m delay and an acousto-optical modulator in one arm of the interferometer. The obtained frequency noise spectrum is shown in Fig. 3. At high frequencies, we can spot the beginning of the white frequency noise region at $0.06\text{Hz}^2/\text{Hz}$ starting from 500kHz from which we measure a Lorentzian linewidth (corresponding to the intrinsic noise of the source) of about $\Delta\nu_{Lorentz} = 0.06\pi \approx 0.2$Hz which agrees well with the specifications. We also emphasize on the increased noise at low frequencies that impacts the quality of the phase measurements at long distances and the higher the effective laser linewidth is. The longer the observation window, the more low-frequency added phase noise [18]. Indeed, as we are computing differential phases, we need a stable phase reference which translates into a high-coherence requirement for the laser. Ideally, the phase observed by the probing signal at the modulation step and the one that is added by the local oscillator at the coherent mixer on the receiver side should be the same.

V. Experimental results

A. Phase noise limit

First, we perform measurements in static conditions (no disturbances applied through the actuators) with codes of length $T_{code} = 2.62$ms or equivalently 2^{17} bits. The phase standard deviation StDv measured over an observation window of 1s is shown as a function of distance in Fig. 4 (bold red line). We notice an exponential growth of phase noise towards 45km and beyond. An exponential growth of the phase StDv is also forecast from the numerical simulation shown for different laser linewidth values, leading to a challenging identification of mechanical events over long distances. Perturbations impacting the fibre with a very-high energy only can be detected at long distances with a fixed probing code length, i.e. a fixed targeted mechanical bandwidth. Indeed, any OTDR-based DAS interrogation scheme has a trade-off between sensitivity, bandwidth and reach. In our case, one way of overcoming phase noise at long distances would be an averaging over several interrogation codes, however this limits the mechanical bandwidth of the detectable events because the refresh rate of the estimated phase information would be diminished.

We observe that the experimental phase StDv over the fibre distance is well fitted by the model when considering a phase noise of a laser with an equivalent Lorentzian linewidth around 75Hz. This is understandable when we look at the measured frequency noise spectrum of the used laser. At a short distance, a correct fit is obtained for all simulated laser linewidth values but the further the signal propagates from the interrogator, the more vulnerable the phase estimation to low-frequency non-white noise.

B. Multi-resolution event localization

We introduce a multi-tone perturbation at 0.9km from the interrogator. To avoid a permanent monitoring of all fibre segments at $S_r = 2$m corresponding to $F_s = 50$MBaud, we start by processing the differential phases from the highest-intensity segment each $L = 250$ adjacent ones. On the left part of Fig. 5, we show the selected highest-reflecting

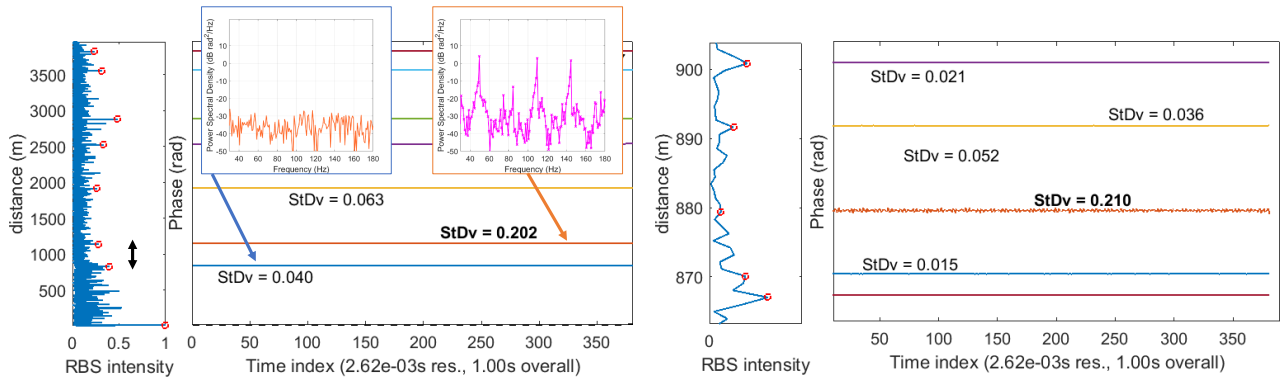

Fig. 5. Multi-resolution event localization. Left part: initial coarse-resolution monitoring showing Rayleigh Back-Scattered (RBS) intensity as a function of distance & phase evolution at selected best segments each 500m. Right part: second-stage monitoring with a finer selection each 16m over a smaller section (highlighted by a double-ended arrow line on the left) bounded by the position of the detected alarm (inset in orange) and the preceding alarm-free position.

segments over the first four kilometers and the evolution of the corresponding differential phase over one second. The used T_{code} is fixed at 2.62ms. The perturbation induced by the actuator is easily detected using an energy criterion, as shown through the power spectral densities of the phases in the insets of Fig. 5, at an average resolution $S_{coarse} = 250S_r = 500$m. The initial detected position is 1100m. A new selection process is activated locally over the segment preceding the detected alarm using an enhanced resolution $S_{fine} = 4S_r = 8$m (random value chosen for illustration). A new localization result at 879m is shown on the right with a better accuracy. This multi-resolution approach is capable of handling several alarms in parallel over all the sensed fibre by refining the localization in an iterative way, thus saving computation efforts compared with a permanent monitoring at the native gauge length.

C. Recognition of a synthetic engine noise

Phase noise limits at several distances were measured in [19] through the recognition of a single tone perturbation. It was found that a 40nm peak-to-peak perturbation was still detectable when applied on the fibre at 25km from the interrogator. In this section, we demonstrate the detection of more complex signals emulating vibrations generated by vehicle engines. A three-tone signal at 50, 105 and 145Hz is selected and its power spectral density is shown in Fig. 7 (dotted line).

We apply the same signal through the two actuators located at 1 and 51km respectively from the interrogation unit. The probing code length is $T_{code} = 2.62$ms yielding a bandwidth of $BW = 193$Hz. Following the data processing described in section II, the differential phase StDv between a subset of segments separated by $S_{coarse} = 150$m to detect and localize the events along the line. Fig. 6 shows the measured phase StDv as a function of the fibre distance. The two mechanical events appear as two StDv peaks at the expected locations. The phase evolution over the 1s measurement window is also displayed in the insets of Fig. 6 for each of the two detected peaks locations.

In Fig. 7, we plot the power spectral density (PSD) of the differential phase at the locations of the two StDv peaks. The

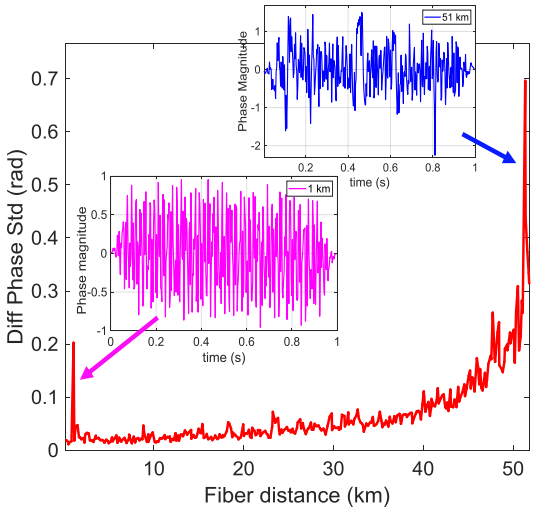

Fig. 6. Measured standard deviation of the differential phase along the fibre with an engine noise perturbation injected at 0.9 and 51km. Insets show the time evolution of the phases at the perturbed locations.

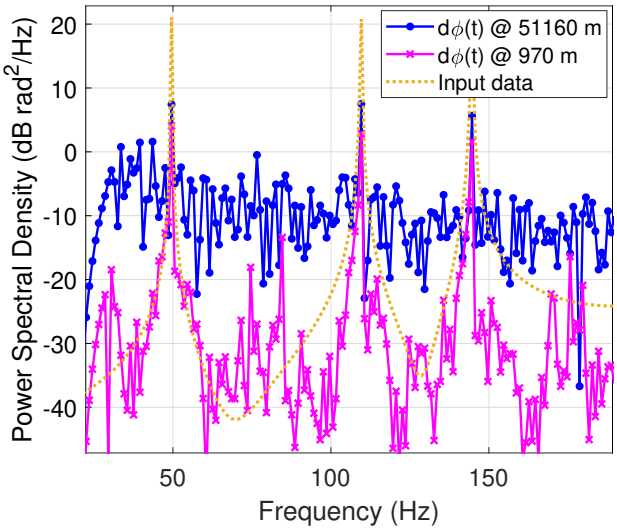

Fig. 7. Power spectral densities (PSD) of phase variations at detected event locations compared to the PSD of the applied vibration signal

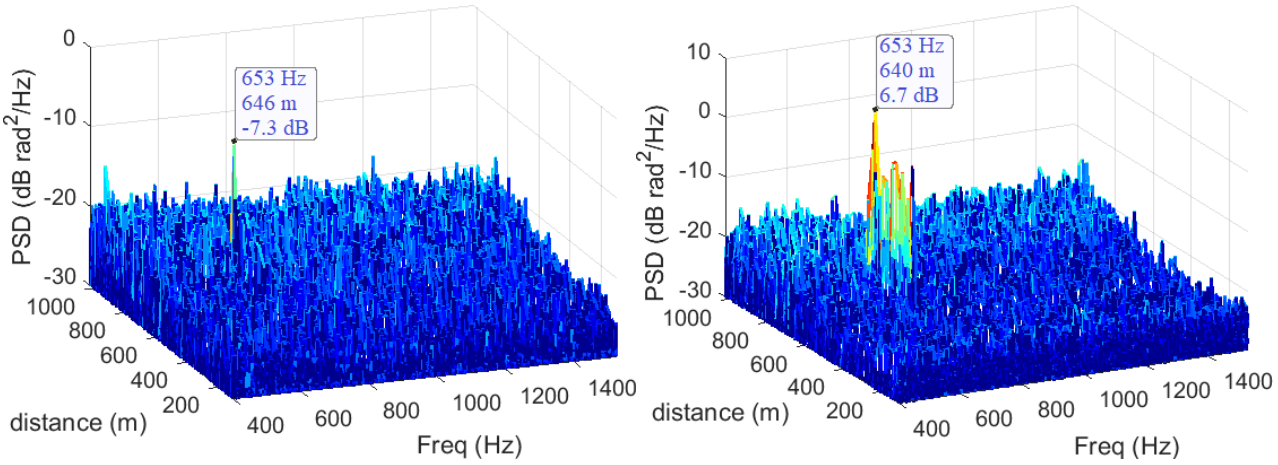

(a) Measured level at the fibre location: 68dB SPL

(b) Measured level at the fibre location: 88dB SPL

Fig. 8. Detection of a 653Hz pure tone, acoustically generated 0.8m away from the fibre cable at 640m distance.

spectral signature of the engine noise at the first location (1km) is well preserved, with a signal-to-noise ratio (SNR) of 30dB approximately. After 51km, the enhanced phase noise resulting from the increased loss of coherence of the laser source reduces the SNR to 10dB roughly, however the recognition of the mechanical event is still possible even after a round-trip propagation over $51km$ of SSMF. We also notice the higher peak power levels detected at 51km, in line with the longer coiled fibre length at this location (133cm at 51km versus 55cm at 1km corresponding to a difference of 3.8dB).

D. Perspectives and on-site experiment

The above results were achieved with mechanical excitations directly applied to the fibre by means of piezo actuators. This technique is advantageous to handle the exact position where the perturbation reaches the fibre and also to quantitatively relate the optical phase change to the magnitude of the mechanical perturbation.

For practical situations, the excitation sources (vehicules, machineries, pedestrians...) are rather located a few meters away from the fibre cable deployed by the telecom operator. The fibre is perturbed by vibrations or by acoustic waves over a distance and with an attenuation which is strongly environment-dependent. This situation makes quantitative measurements potentially difficult to achieve in the field and the extrapolation of the results to other environment questionable.

However, we describe for illustration an experimental study carried out in a corridor of building. An SMF cable is deployed in a crawl space 0.8m below the floor and connects two laboratories separated by 100m. A first 600m SMF spool precedes the 100m deployed cable whereas a 320m spool terminates the link, leading to a 1020m long fibre under test. The setup is tuned to capture perturbations over a 1500Hz bandwidth and with a 2m gauge length (50MBaud symbol rate, $T_{code} = 328\mu s$ or equivalently 2^{14} bits). An acoustic perturbation is generated at 640m from the fibre start by means of a loudspeaker positioned on the floor that generates a 653Hz pure tone. The tone is emitted from the loudspeaker at various power levels and the related sound pressure level at the fibre cable closest vertical position in the crawl space is measured by means of a sound level meter. Figures 8a and 8b display the PSD of the phase variations captured along the fibre within a 2-second period when the Sound Pressure Level (SPL) at the fibre side is equal to 68 and 88dB_{SPL} respectively. The differential phase is processed over a subset of segments that yields a 15m coarse spatial resolution. The spectral display starts from 400Hz to get rid of low frequency noises induced by air conditioning machinery located in the building part under test. Fig. 8a highlights that the 68dB_{SPL} pure tone is detected at an estimated position of 646m from the fibre start, roughly 15dB above the phase noise observed in the distance versus frequency plane. When the acoustic waveform reaches the fibre with a sound pressure level of 88dB_{SPL}, the pure tone is now detected at 640m and 39dB above the noise level. We do not exactly retrieve the 20dB pressure level difference between the 2 measurements, mainly due to the spatial resolution of the analysis. In addition, it can be observed that the 653Hz tone is not simply detected at the fibre position the closest to the loudspeaker, but over a wider distance along the fibre. The reason is that the high-level excitation of the latter test induces an acoustic radiation in the crawl space below the corridor, thus also affecting fibre cable segments located some tenths of meters away from the loudspeaker position. On the other hand, the acoustic radiation spreads less after 640m. This can be explained by the presence of a reinforced concrete wall at approximately 700m separating the crawl space below the corridor in which the loudspeaker is located from the rest of the floor. This wall strongly attenuates the generated acoustic perturbation, hence the portion of the sensed fiber cable that goes through this wall into another crawl space is much less impacted. This complementary experimental study proves the ability to detect, localize and identify acoustic perturbations of various pressure levels by means of a standard SMF cable deployed in a building.

VI. Conclusion

We studied in this work the performance of a novel polarization-multiplexed coded probing method for vibration sensing applications. A long-distance sensing capability over standard telecom fibres was demonstrated. The use of a dual-polarization coherent receiver along with the designed codes enabled a perfect estimation of the fibre response. Noise limits were modeled and measured proving that the loss of coherence of the laser source is the limiting phase noise for this technique. Furthermore, we described a low-complexity monitoring approach that enables scaling-up the sensing method to finer spatial resolutions through a multi-resolution iterative implementation. Mechanical events, made of a sum of three tones emulating an engine noise, were detected, localized and identified from a spectral analysis over a fibre distance that exceeds 50km. The study was complemented for illustration purposes by practical test cases performed in a building using a deployed telecom fibre. These results set the stage for new applications of fibre sensing over existing telecom infrastructure for smart city monitoring and safety applications.

Acknowledgment

The authors would like to thank Loïc Morvan and Christian Larat from Thales Research & Technology for the measurement of the frequency noise spectrum of the ultra-narrow-linewidth OEwaves$^{\mathrm{TM}}$ laser.

References

[1] G. A. Wellbrock, T. J. Xia, M. Huang, Y. Chen, M. Salemi, Y. Huang, P. Ji, E. Ip, T. Wang, "First Field Trial of Sensing Vehicle Speed, Density, and Road Conditions by Using fibre Carrying High Speed Data," Optical fibre Conference, San Diego, California, March 2019

[2] G. Cedilnik, R. Hunt, and G. Lees, "Advances in Train and Rail Monitoring with DAS," in 26th International Conference on Optical fibre Sensors, OSA Technical Digest (Optical Society of America, 2018), paper ThE35.

[3] G. Marra et al., "Ultrastable laser interferometry for earthquake detection with terrestrial and submarine cables," Science 10.1126/science.aat4458 (2018)

[4] M. E. Froggatt and D. K. Gifford, "Rayleigh backscattering signatures of optical fibres—Their properties and applications," 2013 Optical fibre Communication Conference and Exposition and the National fibre Optic Engineers Conference (OFC/NFOEC), Anaheim, CA, 2013, pp. 1-3.

[5] R. Juskaitis, A. M. Mamedov, V. T. Potapov, and S. V. Shatalin, "Interferometry with Rayleigh backscattering in a single-mode optical fibre," Opt. Lett. 19, 225-227 (1994)

[6] Y. Wang, B. Jin, Y. Wang, D. Wang, X. Liu and Q. Bai, "Real-Time Distributed Vibration Monitoring System Using Φ -OTDR," in IEEE Sensors Journal, vol. 17, no. 5, pp. 1333-1341, 1 March1, 2017.

[7] Arthur H. Hartog, "An introduction to distributed optical fibre sensors," Chapter 6, sections 6.2,6.3 and 6.7, CRC Press, Taylor & Francis group, 2017

[8] G. Yang, X. Fan, S. Wang, B. Wang, Q. Liu, Z. He, "Long-range distributed vibration sensing based on phase extraction from phase-sensitive OTDR," IEEE Photonics Journal, 2016, vol. 8, no 3, p. 1-12

[9] C. Dorize and E. Awwad, "Enhancing the performance of coherent OTDR systems with polarization diversity complementary codes," Optics Express, vol. 26, pp. 12878-12890, May 2018

[10] H. F. Martins, K. Shi, B. C. Thomsen, S. Martin-Lopez, M. Gonzalez-Herraez, and S. J. Savory, "Real time dynamic strain monitoring of optical links using the backreflection of live PSK data," Opt. Express 24, 22303-22318 (2016)

[11] E. Awwad, C. Dorize, P. Brindel, U. Bertuzzi, J.Renaudier, G. Charlet, "Large Bandwidth Phase-Sensitive DAS with Novel Polarization-Multiplexed Probing Technique," Optical fibre Sensors Conference, Lausanne, Switzerland, September 2018

[12] C. Dorize, E. Awwad, S. Guerrier, J. Renaudier, "Vibration identification over 50km SSMF with Pol-Mux coded phase-OTDR," European Conference on Optical Communications, paper W.1.E.1, September 2019

[13] G. Cranch and P. Nash, "High-Responsivity fibre-Optic Flexural Disk Accelerometers," J. Lightwave Technol. 18, 1233- (2000)

[14] E. Awwad, C. Dorize, and J. Renaudier, "Efficient Multi-Event Localization from Rayleigh Backscattering in Phase-Sensitive OTDR Systems," in Optical Sensors and Sensing Congress (ES, FTS, HISE, Sensors), OSA Technical Digest (Optical Society of America, 2019), paper EW6A.2.

[15] S. Guerrier, C. Dorize, E. Awwad, and J. Renaudier, "A dual-polarization Rayleigh backscatter model for phase-sensitive OTDR applications," Optical Sensors and Sensing Conference, San José, California, June 2019

[16] L. B. Liokumovich, N. A. Ushakov, O. I. Kotov et al., "Fundamentals of optical fibre sensing schemes based on coherent optical time domain reflectometry : Signal model under static fibre conditions," J. Lightwave Technology, Sep. 2015, vol. 33, pp. 3660-3671

[17] Arthur H. Hartog, "An introduction to distributed optical fibre sensors," Chapter 2, section 2.1.2.2 (reference [28]), CRC Press, Taylor & Francis group, 2017

[18] Gianni Di Domenico, Stéphane Schilt, and Pierre Thomann, "Simple approach to the relation between laser frequency noise and laser line shape," Appl. Opt. 49, 4801-4807 (2010)

[19] C. Dorize, E. Awwad and J. Renaudier, "High Sensitivity φ -OTDR Over Long Distance With Polarization Multiplexed Codes," in IEEE Photonics Technology Letters, vol. 31, no. 20, pp. 1654-1657, 15 Oct.15, 2019.